

Squeezing Edge Performance: A Sensitivity-Aware Container Management for Heterogeneous Tasks

Yongmin Zhang, *Senior Member, IEEE*, Pengyu Huang, Mingyi Dong, Jing Yao

Abstract—Edge computing enables latency-critical applications to process data close to end devices, yet task heterogeneity and limited resources pose significant challenges to efficient orchestration. This paper presents a measurement-driven, container-based resource management framework for intra-node optimization on a single edge server hosting multiple heterogeneous applications. Extensive profiling experiments are conducted to derive a nonlinear fitting model that characterizes the relationship among CPU/memory allocations and processing latency across diverse workloads, enabling reliable estimation of performance under varying configurations and providing quantitative support for subsequent optimization. Using this model and a queueing-based delay formulation, we formulate a mixed-integer nonlinear programming (MINLP) problem to jointly minimize system latency and power consumption, which is shown to be NP-hard. The problem is decomposed into tractable convex subproblems and solved through a two-stage container-based resource management scheme (CRMS) combining convex optimization and greedy refinement. The proposed scheme achieves polynomial-time complexity and supports quasi-dynamic execution under global resource constraints. Simulation results demonstrate that CRMS reduces latency by over 14% and improves energy efficiency compared with heuristic and search-based baselines, offering a practical and scalable solution for heterogeneous edge environments with dynamic workload characteristics.

Index Terms—Edge computing, resource management, container configuration, heterogeneous tasks.

I. INTRODUCTION

The rapid proliferation of Internet of Things (IoT) technologies has driven the deployment of latency-sensitive applications, including augmented reality (AR), autonomous driving, and smart healthcare [1]. These applications require stringent Quality of Service (QoS) guarantees, such as ultra-low latency, high reliability, and energy efficiency. However, conventional cloud computing architectures based on centralized processing often fail to satisfy these requirements due to significant backhaul transmission delay and limited scalability [2]. To address these limitations, edge computing has emerged as a promising paradigm, placing computational resources in close proximity to data sources. By reducing data transmission delays and enabling localized computation, edge computing significantly enhances QoS metrics, positioning it as a critical enabler for modern intelligent systems [3].

Despite its advantages, edge computing faces notable challenges in resource optimization due to the limited computational and storage capacities of individual edge servers. Existing research has primarily addressed network-wide resource

Y. Zhang, P. Huang, M. Dong, and J. Yao are with the School of Computer Science and Engineering, Central South University, Changsha, 410083, China. E-mails: {zhangyongmin, huangpengyu, dongmingyi, jingyao}@csu.edu.cn.

utilization through inter-server collaboration strategies, such as task offloading, load balancing, and predictive scheduling [4]–[8]. While these methods enhance coordination among distributed nodes, they often overlook the problem of how to orchestrate resources within a single resource-constrained edge server hosting multiple applications. In such settings, naive or static policies can assign disproportionate CPU and memory resources to latency-insensitive workloads, leaving latency-critical tasks underprovisioned and degrading overall QoS [9], [10]. This mismatch motivates a resource management framework that not only preserves service quality but also squeezes as much performance as possible out of limited edge resources by reallocating CPU and memory according to task-specific resource sensitivities.

A central challenge in edge resource optimization lies in task heterogeneity, which refers to the diverse resource requirements and sensitivities of tasks to computational resources. Unlike homogeneous workloads, edge applications can differ drastically in how their latency responds to changes in CPU, memory, and concurrency levels, even when running on the same hardware and container runtime environment [9]. For example, memory-intensive workloads may experience significant performance degradation when memory is reduced, whereas some compute-oriented models are more resilient under similar conditions [11]. In this paper, we mainly focus on heterogeneity in the CPU and memory demands and sensitivities of applications under a given hardware platform. We refer to these differences in how latency responds to resource adjustments as the resource sensitivity of an application. Without sensitivity-aware allocation, misconfigurations can easily lead to performance bottlenecks, increased energy consumption, and degraded QoS.

Moreover, task heterogeneity also interacts with system-level constraints in a nontrivial manner. When multiple containerized applications share a single edge server, the limited CPU and memory resources couple their performance: improving the latency of one application often requires reducing resources for others. As a result, system performance depends critically on how container quotas are chosen under shared resource constraints, and naive utilization-based scaling or single-resource heuristics often fail to achieve balanced efficiency across heterogeneous workloads. Our measurement-driven fitting results in Section III further show that the latency response to CPU and memory adjustments is highly nonlinear and application dependent, indicating that simple threshold rules cannot adequately capture the underlying behavior. These observations motivate a sensitivity-aware container management strategy that exploits heterogeneity in delay–resource

elasticity, reallocating CPU and memory from low-elasticity workloads to high-elasticity ones to squeeze more performance from a resource-constrained edge server.

To address these issues, this paper presents a dynamic container-based resource management framework for a single resource-constrained edge server that hosts multiple container clusters. The goal is to jointly determine the number of containers and their CPU and memory quotas under shared resource constraints. Based on extensive profiling across heterogeneous applications, we derive a measurement-driven performance model capturing the nonlinear relationship among resource allocations and processing latency. Leveraging this model, we formulate a mixed-integer nonlinear optimization problem to minimize both latency and energy consumption, and design a sensitivity-aware resource management scheme to achieve efficient intra-node resource orchestration. Our main contributions are summarized as follows:

- We construct a container-based fitting function that captures the relationship between processing delay and resource configurations (CPU and memory) for heterogeneous tasks, and use it to characterize the heterogeneous resource sensitivities of different applications.
- We formulate the resource management problem as a joint optimization of processing latency and energy consumption, modeled as a MINLP problem, and propose a sensitivity-aware container-based resource management scheme (CRMS) to derive near-optimal allocation strategies under latency–energy trade-offs.
- Extensive simulations show that the proposed scheme effectively adapts to diverse workload patterns, reducing average response latency by at least 14% compared to traditional search algorithms.

The remainder of this paper is organized as follows. Section II reviews related works. Section III presents the measurement-driven container-based performance model and profiling methodology. Section IV introduces the system architecture, power consumption model, processing delay model, and formulates the resource management optimization problem. Section V describes the proposed server resource management scheme and the derivation of optimal container configurations based on theoretical analysis. Section VI provides extensive simulation results to evaluate the scheme’s effectiveness. Finally, Section VII concludes the paper.

II. RELATED WORK

Efficient resource allocation is fundamental to ensuring service quality on resource-constrained edge servers. A wide spectrum of approaches has been investigated—from heuristic autoscaling and analytical modeling to learning-based and serverless frameworks. This section reviews these studies from a methodological perspective, focusing on rule-based analytical models, heterogeneity-aware optimization, and hybrid or serverless architectures. It further highlights their limitations in managing heterogeneous task workloads.

Early studies primarily focused on optimizing resource usage for homogeneous or predictable tasks. Threshold-based methods [4]–[6] adjust CPU or memory allocations when

metrics exceed predefined limits. However, such thresholds lack the flexibility needed for tasks that demand simultaneous scaling of multiple resources, often resulting in resource bottlenecks. Queue-theoretic approaches [12], [13] model task arrivals and service rates to minimize average response time. While effective for homogeneous tasks, these methods are insufficient for prioritizing latency-critical tasks in heterogeneous environments. Predictive methods [14]–[16] forecast future demands using historical data, but their prediction accuracy significantly degrades when task characteristics and resource demands become unpredictable. These limitations highlight the need for adaptability and sensitive-aware strategies in heterogeneous edge environments.

A second line of work explicitly addresses task heterogeneity through dynamic prioritization and resource partitioning. Sharif *et al.* [17] proposed A-PBRA, a method that classifies tasks based on resource sensitivity (e.g., CPU-bound vs. memory-bound) and allocates resources accordingly. He *et al.* [18] introduced a three-stage model (TSHC) to jointly optimize task offloading and resource allocation under deadline constraints, yet its reliance on a centralized scheduler limits scalability in distributed edge environments. Control-theoretic methods [19]–[21] dynamically adjust resources via feedback loops, but their reliance on pre-defined performance models limits flexibility for unseen task types. Reinforcement learning (RL) [22], [23] learns allocation policies without relying on explicit modeling, but the high training overhead and slow convergence of RL limit its applicability in real-time scenarios with bursty, heterogeneous workloads.

To balance flexibility with efficiency, hybrid architectures have emerged. Han *et al.* [24] decoupled task scheduling from resource provisioning via a hierarchical framework, enabling differentiated handling of tasks. Ascigil *et al.* [25] compared centralized versus decentralized allocation, showing that partial coordination improves deadline compliance for mixed-criticality tasks. In serverless edge environments, Raza *et al.* [26] used Bayesian optimization to tune resource configurations per function type, while Safaryan *et al.* [27] optimized memory allocations by tracing inter-function dependencies. However, these solutions optimize isolated resources or assume predictable task workflows, neglecting the necessity of coordinated multi-resource adaptation.

Overall, existing approaches either optimize isolated metrics, rely on static performance models, or incur substantial online learning costs, which makes them difficult to apply directly to fine-grained CPU and memory quota management for heterogeneous containerized workloads on a single edge node. In this work, we take a complementary approach by focusing on intra-node resource management and developing a lightweight, measurement-driven scheme that builds a container-level performance model and periodically re-optimizes CPU and memory quotas, as well as the number of containers, across heterogeneous workloads, without requiring online learning or frequent retraining.

III. CONTAINER-BASED PERFORMANCE MODEL

In this section, we build a container-based performance model that maps allocated CPU and memory to the average

processing delay of each application. This empirical latency-resource function provides a foundation for the subsequent processing delay model and resource optimization.

A. Modeling Motivation

Docker containers have been widely deployed on edge servers to process heterogeneous tasks, thanks to their advantages, including short startup time, low memory overhead for encapsulating applications, and elastic scalability [28]. As a result, dynamic resource management in edge computing can be achieved by controlling the resource configurations of Docker containers on the edge server. Most existing research related to Docker containers [28]–[30] assumes that resource allocations are fixed or that processing rates scale linearly with task size. However, without considering the heterogeneity and resource demands of tasks, this assumption may not hold for edge servers processing heterogeneous workloads.

To verify this assumption, we consider image classification and object detection as two representative categories of heterogeneous tasks. By deploying various models from these two categories in Docker containers, we conduct extensive profiling experiments to examine how processing latency varies with different CPU and memory configurations. The resulting measurements serve as the foundation for constructing the container-based performance model presented in this section.

B. Experimental Setup

The experiments are conducted using Docker Swarm as the container orchestration tool. Image processing applications are deployed with PaddlePaddle official images to simulate heterogeneous tasks. Four representative applications are tested: ResNet_v2, SE_ResNeXt, and MobileNet_v2 for image classification, and SSD_MobileNet_v1 for object detection. The CPU and memory resources are controlled by the Docker parameters `--cpus` and `-m`, which specify the maximum CPU quota and memory allocation, respectively.

By continuously sending image processing requests to the application containers, we measure the average processing delay under each resource configuration. In each experiment series, we fix one resource (CPU or memory) to a sufficiently large value and vary the other over a set of discrete configurations, so that the individual impact of CPU and memory on processing latency can be characterized separately.

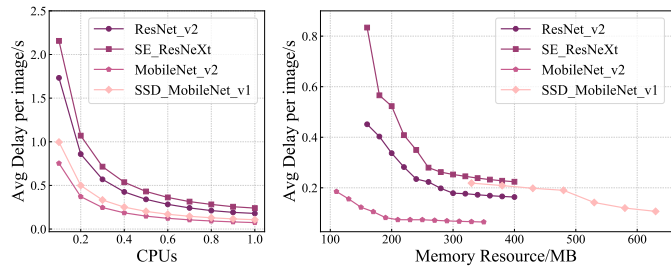


Fig. 1. Impact of CPU and memory allocations on processing delay.

C. Profiling Observations

We control container resources via Docker runtime parameters. Specifically, `--cpus` sets a CPU time *limit* via the CFS quota/period mechanism (allowing fractional capacity, e.g., `--cpus=1.5`), while `-m` sets a hard memory limit. In our profiling, we vary these two parameters to obtain latency measurements under different CPU and memory configurations.

When memory resources are unrestricted, we evaluate how processing latency varies with CPU allocation across four applications, as shown in Fig. 1(a). The results reveal a non-linear increase in latency as the available CPU capacity decreases. Moreover, the degree of sensitivity to CPU resources differs markedly among applications: SE_ResNeXt is most sensitive to CPU reduction, followed by ResNet_v2, MobileNet_v2, and SSD_MobileNet_v1. These results highlight the importance of fine-grained CPU allocation tailored to each application's computational demand.

Conversely, when CPU resources are unrestricted, we investigate the effect of memory allocation on processing latency for the same four applications, as shown in Fig. 1(b). The SSD_MobileNet_v1 object detection model exhibits the highest memory requirement, while MobileNet_v2 shows a similar but less pronounced trend. In contrast, ResNet_v2 and SE_ResNeXt are more sensitive to memory reductions, where even small decreases lead to sharp increases in latency. A clear lower bound is also observed: when memory allocation falls below a threshold, the container terminates due to an Out-of-Memory (OOM) error. This empirical observation underscores that both CPU and memory are performance-critical resources, and adequate memory provisioning is essential for stable container execution.

Based on these observations, for each application i , we define a minimum feasible memory r_i^{\min} as the smallest allocation that avoids OOM events, and a saturation point r_i^{\max} beyond which additional memory yields negligible latency improvement. These empirically derived bounds are later used to constrain the feasible region in the optimization model. Fig. 1 illustrates that heterogeneous tasks have distinct demand characteristics for CPU and memory resources, which contradicts the assumption that the processing rate is a linear function of task size. To further explore the relationship between processing delay and resource configuration, i.e., CPU and memory, we further construct a container-level performance model of processing latency as a function of CPU and memory resources in the next subsection.

D. Model Fitting and Validation

We conduct latency profiling for four applications under various CPU and memory configurations. To reduce noise and measurement errors, each data point represents the average of multiple valid runs, yielding stable results for curve fitting. Based on the collected data, we fit a container-level latency-resource function $d_i(r_i^{\text{cpu}}, r_i^{\text{mem}})$ for each application i . Using the SciPy toolkit, we perform non-linear least squares fitting across five candidate models, evaluated by the Root Mean Square Error (RMSE). A smaller RMSE indicates a closer match between predicted and measured latency. The RMSE

TABLE I
RMSE AND R-SQUARE COMPARISON OF CANDIDATE FITTING FUNCTIONS.

Function Model	ResNet_v2		SE_ResNeXt		MobileNet_v2		SSD_MobileNet_v1	
	RMSE	R-Square	RMSE	R-Square	RMSE	R-Square	RMSE	R-Square
$\frac{\kappa_1}{1-e^{-\kappa_2 r_i^{cpu}}} + e^{\frac{\kappa_3}{r_i^{mem}}}$	2.69	0.99	4.17	0.99	0.72	0.99	2.79	0.99
$\frac{\kappa_1}{r_i^{cpu}} + \kappa_2 (r_i^{mem})^2 + \kappa_3 r_i^{mem}$	4.17	0.99	5.77	0.99	1.94	0.99	1.95	0.97
$\frac{1}{\kappa_1 \log(1+r_i^{cpu}) + \kappa_2 \log(1+r_i^{mem})}$	7.41	0.97	12.10	0.95	3.32	0.97	4.84	0.97
$\frac{\kappa_2 + \kappa_3 (r_i^{cpu})^2 + \kappa_4 (r_i^{mem})^2}{\kappa_1^3}$	14.88	0.89	21.84	0.85	6.15	0.91	8.61	0.91
$\kappa_1 (r_i^{cpu})^3 + \kappa_2 (r_i^{mem})^3 + \kappa_3 r_i^{cpu} r_i^{mem}$	23.31	0.74	28.12	0.76	10.88	0.71	15.33	0.70

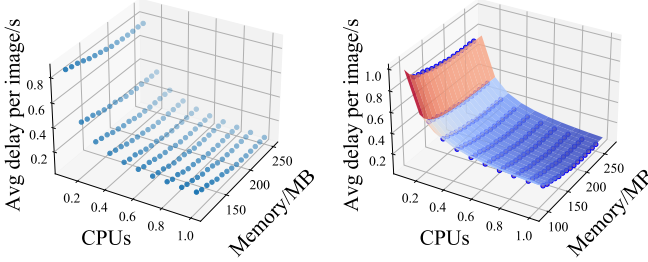


Fig. 2. Fitted latency–resource surfaces versus measured data.

and R^2 values for all candidates are listed in Table I, from which Eq. (1) achieves the best fit and is therefore adopted to model the average processing delay of application i :

$$d_i = \frac{\kappa_{i,1}}{1 - e^{-\kappa_{i,2} r_i^{cpu}}} + e^{\frac{\kappa_{i,3}}{r_i^{mem}}}, \quad (1)$$

where r_i^{cpu} and r_i^{mem} denote the CPU and memory resources allocated to the container for application i . The parameters $\kappa_{i,1} < 0$, $\kappa_{i,2} > 0$, and $\kappa_{i,3} > 0$ are the fitted coefficients obtained from the non-linear regression. These coefficients capture each application’s sensitivity to CPU and memory allocations. Intuitively, a larger $\kappa_{i,2}$ makes the first term more responsive to changes in r_i^{cpu} , while a larger $\kappa_{i,3}$ amplifies the effect of r_i^{mem} in the exponential term. The subsequent resource management scheme exploits these heterogeneous sensitivities when redistributing CPU and memory under global constraints.

To validate the suitability of Eq.(1), we compare its fitted latency surface with actual measurements from the MobileNet_v2-based image classification application under varying CPU and memory configurations. The scatter points align closely with the model’s predicted surface, indicating that the fitting function in Eq.(1) accurately captures the observed latency trends. This close alignment supports the choice of Eq.(1) as the performance model to characterize the relationship between processing delay, CPU, and memory resources. This initial observation based on RMSE suggests that the model is relatively reasonable.

To further assess the fitting quality of Eq. (1) for the MobileNet_v2 model, we examine the residual and Q–Q plots shown in Fig. 3, which offer additional insights into the model’s accuracy. The residual plot demonstrates that the residuals are randomly distributed, indicating a good fit without systematic bias. The QQ plot reveals that the residuals align closely with the 45-degree reference line, suggesting that they approximate a normal distribution, which is desirable for

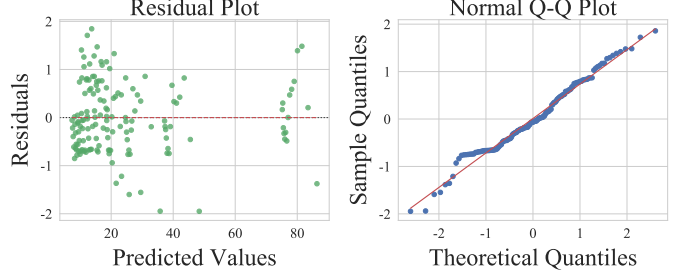


Fig. 3. Residual and Q–Q plots verifying the performance model fitting.

model accuracy. Additionally, the adjusted R-squared value is exceptionally high at 0.9987, indicating that the model accounts for nearly all the variability in the data. The mean squared error (MSE) of 0.5568 and root mean squared error (RMSE) of 0.7223 further reflect the model’s high predictive accuracy, underscoring its robustness in capturing the relationship between CPU/memory configurations and inference latency. Collectively, these metrics confirm that Eq. (1) is an effective and reliable choice for modeling the inference latency, providing a strong foundation for further optimization and analysis.

IV. SYSTEM MODEL

In this section, we present a container-based resource management framework for a single edge server, as illustrated in Fig. 4. The server hosts multiple containerized applications with heterogeneous workload characteristics. These include distinct request arrival rates, varying average request sizes (measured by the number of images per request), and diverse latency–resource sensitivities as modeled in Section III. The framework focuses on efficient intra-node management of CPU and memory resources within Docker container clusters by coordinating monitoring, scheduling, and allocation.

IoT devices, including sensors, traffic cameras, and smartphones, generate requests that are transmitted over wireless links to the edge server for computation. Let $\mathcal{M} = \{1, 2, \dots, m\}$ denote the set of applications hosted on the server. For application $i \in \mathcal{M}$, the edge server maintains a container cluster with N_i homogeneous containers. Each incoming request of application i is processed by one container instance. Within each container, requests follow a First-Come-First-Serve (FCFS) scheduling policy. The average request size of application i , defined as the mean number of images per request, will later be used to relate the service rate to the per-image latency.

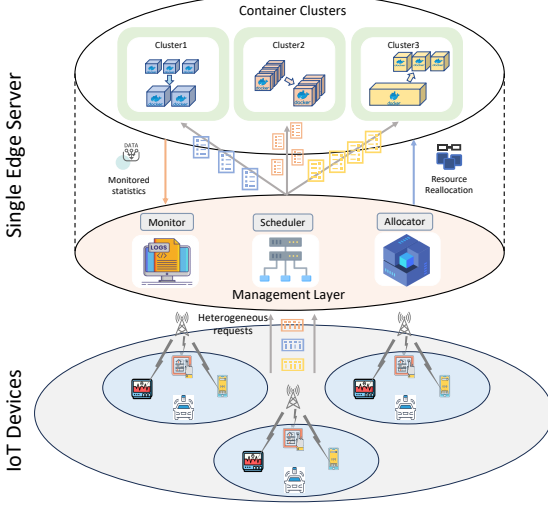


Fig. 4. Architecture of the container-based resource management framework within a single edge server.

The system is logically divided into a management plane and a worker plane. The worker plane runs the container clusters and executes the application requests. The management plane consists of three functional modules: the monitor, scheduler, and the allocator, which cooperate to achieve dynamic resource management. The monitor continuously collects runtime statistics, including request arrival rates, average processing delays, and container resource configurations, to capture significant workload variations. Using the monitoring information, the scheduler assigns incoming requests to the corresponding application clusters according to their types, ensuring proper task routing without altering resource quotas. The allocator updates container configurations in response to workload variations detected by the monitor: it performs horizontal scaling by adjusting the number of containers N_i and vertical scaling by adjusting the CPU and memory quotas (r_i^{cpu}, r_i^{mem}) of each application. The exact triggering policy of resource reconfiguration (periodic or on-demand) is implementation-dependent and not the focus of this study; here we assume the allocator reacts when the monitor reports material workload changes.

To evaluate and optimize system performance, two quantitative models are introduced in the following subsections: a power consumption model and a processing delay model. The former relates container resource allocations to the incremental power attributable to applications at the edge server, while the latter estimates the per-image latency of each application given its container-level CPU and memory configuration. These models provide the foundation for the resource management optimization problem developed subsequently.

A. Power Consumption Model

Different from existing power models that parameterize server power as a function of CPU frequency and chip-level energy coefficients, we model power as a function of the allocated CPU capacity. This design choice aligns with container orchestration mechanisms, where the adjustable resource control is the CPU quota rather than processor frequency.

Following the modeling principle in [31], the dynamic power consumption is approximated as a linear function of the allocated CPU quota. We define the incremental power of application i as:

$$\Delta P_i = (P^{full} - P^{idle}) U_i^{cpu}, \quad (2)$$

where P^{idle} and P^{full} are the measured server power at idle and at a reference full-load state, respectively. The server power is thus expressed as $P^{idle} + \sum_i \Delta P_i$, and the constant idle term P^{idle} does not affect the optimization objective, so it is omitted in subsequent analysis. Here U_i^{cpu} denotes the fraction of total CPU capacity allocated to application i :

$$U_i^{cpu} = \frac{N_i r_i^{cpu}}{\bar{R}^{cpu}}, \quad (3)$$

where N_i is the number of containers for application i , r_i^{cpu} is the CPU quota of each container, and \bar{R}^{cpu} is the total CPU capacity of the edge server. This formulation uses the capacity fraction U_i^{cpu} as a practical proxy for the workload-proportional power term, aligning the model with the resource control interface exposed by the container runtime while remaining consistent in spirit with utilization-based power modeling. This model focuses on CPU power, while memory power is not explicitly modeled. In typical edge servers, memory power exhibits much smaller variation compared to that of the CPU under our workload settings. Its effect can therefore be absorbed into the constant terms P^{idle} and P^{full} without loss of generality. Extending the model to include explicit memory power will be considered in future work.

B. Processing Delay Model

We model the request processing of each application as an M/M/N queue, where request arrivals follow a Poisson process with rate λ_i and service times in each container are exponentially distributed with rate μ_i . The expected number of requests in the system (including both the waiting queue and the servers), denoted by $L_s(N_i, \lambda_i, \mu_i)$, is given by

$$L_s(N_i, \lambda_i, \mu_i) = \frac{\left(\frac{\lambda_i}{\mu_i}\right)^{N_i} \frac{\lambda_i}{N_i \times \mu_i}}{N_i! \left(1 - \frac{\lambda_i}{N_i \times \mu_i}\right)^2} \pi_0 + \frac{\lambda_i}{\mu_i}, \quad (4)$$

$$\pi_0 = \left[\sum_{k=0}^{N_i-1} \frac{1}{k!} \left(\frac{\lambda_i}{\mu_i}\right)^k + \frac{\lambda_i^{N_i}}{N_i! \left(1 - \frac{\lambda_i}{N_i \times \mu_i}\right) \mu_i^{N_i}} \right]^{-1} \quad (5)$$

Here, π_0 denotes the probability that there are no requests in the system, and μ_i is the per-container service rate for application i . Considering the latency–resource relationship in Eq. (1), the service rate can be written as:

$$\mu_i = \frac{1}{\bar{x}_i d_i}, \quad (6)$$

where d_i is the average *per-image* processing latency under the allocated CPU and memory, and $\bar{x}_i > 0$ denotes the average number of images contained in one request of application i ; hence $\bar{x}_i d_i$ is the average processing time per request. According to Little’s law, the expected average response time

per request for application i , denoted by $W_s(N_i, \lambda_i, \mu_i)$, can be given by

$$W_s(N_i, \lambda_i, \mu_i) = \frac{L_s(N_i, \lambda_i, \mu_i)}{\lambda_i}. \quad (7)$$

C. Problem formulation

Based on the preceding models, we formulate a container-based resource management optimization problem, which determines the optimal number of containers and their CPU and memory configurations for each application. The objective is to jointly minimize the processing delay and power consumption under resource capacity constraints. The problem is formulated as follows:

$$\mathbf{P}: \min_{N_i, r_i^{cpu}, r_i^{mem}} U_p = \sum_i \left(\alpha W_s(N_i, \lambda_i, \mu_i) + \beta \frac{\Delta P_i}{\lambda_i} \right), \quad (8)$$

$$\text{s.t.} \quad \sum_i N_i r_i^{cpu} \leq \overline{R}^{cpu}, \quad (9)$$

$$\sum_i N_i r_i^{mem} \leq \overline{R}^{mem}, \quad (10)$$

$$r_i^{min} \leq r_i^{mem} \leq r_i^{max}, \quad \forall i \in M. \quad (11)$$

Here, $\alpha > 0$ and $\beta > 0$ are the weight coefficients for delay and energy terms, respectively. $W_s(N_i, \lambda_i, \mu_i)$ denotes the average response time per request of application i , while $\Delta P_i / \lambda_i$ represents the average incremental power consumption per request. Therefore, U_p minimizes the weighted sum of per-request delay and per-request energy across all applications. Constraints (9) and (10) ensure that the total CPU and memory allocations do not exceed the available system capacities \overline{R}^{cpu} and \overline{R}^{mem} , respectively. Constraint (11) bounds the memory assigned to each container, preventing insufficient memory that could trigger the Out-of-Memory (OOM) killer and avoiding excessive memory allocations that starve other applications.

In Problem **P**, N_i is a non-negative integer variable, while r_i^{cpu} and r_i^{mem} are continuous decision variables, making it a mixed-integer nonlinear programming (MINLP) problem [32]. To further characterize its computational complexity, we next present a polynomial-time reduction from the well-known Unbounded Multi-dimensional Knapsack Problem (UMKP), which is NP-hard [33], leading to the following theorem.

Theorem 1: Problem **P** is NP-hard.

Proof: We prove this by reduction from the Unbounded Multi-dimensional Knapsack Problem. Let k_i denote the number of selected items of type i in the UMKP, which is formulated as

$$\max \sum_{i=1}^m k_i v_i, \quad \text{s.t.} \quad \sum_{i=1}^m k_i w_i^{(j)} \leq C^{(j)}, \quad \forall j \in [1, d]. \quad (12)$$

Here, v_i and $w_i^{(j)}$ denote the profit and the j -th resource weight of item i , respectively, and $C^{(j)}$ is the capacity of dimension j .

We construct a special case of Problem **P** as follows. Each application i corresponds to an item type i in the UMKP, and the number of deployed containers N_i corresponds to the number of selected items k_i . The CPU and memory allocations

map to the two-dimensional resource weights, i.e., $r_i^{cpu} = w_i^{(1)}$ and $r_i^{mem} = w_i^{(2)}$, with total capacities $\overline{R}^{cpu} = C^{(1)}$ and $\overline{R}^{mem} = C^{(2)}$. For the objective function, we simplify Problem **P** by setting $\alpha = 0$ and $\beta = 1$, thereby eliminating the delay term and focusing only on the energy term. Assuming a linear incremental power model $\Delta P_i = c_i N_i$, where $c_i > 0$ is a constant, the objective becomes:

$$\min \sum_i \frac{c_i N_i}{\lambda_i}. \quad (13)$$

Since λ_i is the arrival rate of requests for application i , $\frac{c_i N_i}{\lambda_i}$ can be interpreted as the average incremental energy cost per request under this simplified model. To align this minimization problem with the profit-maximization objective of the UMKP, we define $\frac{c_i}{\lambda_i} = -v_i$. Then, we obtain:

$$\min \sum_i \frac{c_i N_i}{\lambda_i} = \min \sum_i (-v_i) N_i = -\max \sum_i v_i N_i.$$

Thus, an optimal solution to this special case of Problem **P** directly yields an optimal solution to the corresponding UMKP instance. Because UMKP is NP-hard [33], Problem **P** is at least NP-hard. Moreover, reintroducing the nonlinear queuing delay term $W_s(N_i, \lambda_i, \mu_i)$ with factorial and exponential expressions further increases the complexity, making the problem non-convex and computationally intractable [34]. ■

Given the NP-hardness of Problem **P**, exact solutions become computationally infeasible for large-scale instances. To address this challenge, we conduct a problem transformation through theoretical analysis and subsequently develop an efficient resource management algorithm tailored to this setting.

V. SENSITIVITY-AWARE CONTAINER RESOURCE MANAGEMENT SCHEME FOR HETEROGENEOUS TASKS

In this section, we transform Problem **P** into tractable subproblems through theoretical analysis and design a sensitivity-aware container management scheme (CRMS) for intra-node resource orchestration on a single edge server.

A. Problem Transformation in Sufficient Resources Condition

To handle the coupling between the container count N_i and the per-container resource quotas (r_i^{cpu}, r_i^{mem}) in Problem **P**, we first analyze per-application optimal configurations under a sufficient-resource assumption, where the global CPU and memory budget constraints in (9)–(10) are temporarily relaxed. Under this assumption, each application can be optimized independently, leading to two decoupled subproblems: **SP1** (per-container quota selection) and **SP2** (container count selection). The resulting configurations characterize the upper-bound resource demand of each application and will later serve as initialization and guidance for the constrained scheme.

For Subproblem **SP1**, when the edge server has sufficient resources, the allocation to each container can be treated

independently. Thus, for application i , $\forall i \in M$, we determine the optimal per-container CPU and memory by solving:

$$\mathbf{SP1:} \min_{r_i^{cpu}, r_i^{mem}} F_i = \alpha D_i + \beta \frac{\Delta p_i}{\lambda_i}, \quad (14)$$

$$\text{s.t. } D_i = d_i \bar{x}_i, \quad (15)$$

$$r_i^{min} \leq r_i^{mem} \leq r_i^{max}, \quad (16)$$

where D_i denotes the average per-request processing delay with $D_i = \bar{x}_i d_i$, and Δp_i denotes the incremental power consumption of one container for application i relative to the idle baseline:

$$\Delta p_i = (P^{full} - P^{idle}) \frac{r_i^{cpu}}{R^{cpu}}. \quad (17)$$

To verify the existence and uniqueness of the optimal solution to Subproblem **SP1**, we analyze the monotonicity and convexity of F_i with respect to r_i^{cpu} and r_i^{mem} , which is given as follows:

Theorem 2: F_i is a monotonically decreasing function with respect to r_i^{mem} and a convex function of r_i^{cpu} and r_i^{mem} .

Proof: Based on Eq.(14), the first derivative of F_i with respect to r_i^{cpu} and r_i^{mem} can be given by

$$\frac{\partial F_i}{\partial r_i^{cpu}} = \frac{\alpha \bar{x}_i \kappa_{i,1} \kappa_{i,2} e^{\kappa_{i,2} r_i^{cpu}}}{(1 - e^{\kappa_{i,2} r_i^{cpu}})^2} + \frac{\beta (P^{full} - P^{idle})}{\lambda_i R^{cpu}}, \quad (18)$$

$$\frac{\partial F_i}{\partial r_i^{mem}} = -\frac{\alpha \bar{x}_i \kappa_{i,3}}{(r_i^{mem})^2} e^{\frac{\kappa_{i,3}}{r_i^{mem}}}. \quad (19)$$

It can be obtained that $\frac{\partial F_i}{\partial r_i^{mem}} < 0$ holds since $\kappa_{i,3} > 0$, which means that F_i is a monotonically decreasing function with respect to r_i^{mem} . The second derivative of F_i with respect to r_i^{cpu} and r_i^{mem} can be given by

$$\frac{\partial^2 F_i}{\partial (r_i^{cpu})^2} = \frac{\alpha \bar{x}_i \kappa_{i,1} \kappa_{i,2}^2 e^{\kappa_{i,2} r_i^{cpu}} (1 - e^{2\kappa_{i,2} r_i^{cpu}})}{(1 - e^{\kappa_{i,2} r_i^{cpu}})^4}, \quad (20)$$

$$\frac{\partial^2 F_i}{\partial (r_i^{mem})^2} = e^{\frac{\kappa_{i,3}}{r_i^{mem}}} \frac{\alpha \bar{x}_i \kappa_{i,3} (2r_i^{mem} + \kappa_{i,3})}{(r_i^{mem})^4}, \quad (21)$$

$$\frac{\partial^2 F_i}{\partial r_i^{cpu} \partial r_i^{mem}} = \frac{\partial^2 F_i}{\partial r_i^{mem} \partial r_i^{cpu}} = 0. \quad (22)$$

Since $r_i^{cpu} > 0$, $1 - e^{2\kappa_{i,2} r_i^{cpu}} < 0$, $\kappa_{i,1} < 0$, $\kappa_{i,2} > 0$, we have that $\frac{\partial^2 F_i}{\partial (r_i^{cpu})^2} > 0$. Besides, $\frac{\partial^2 F_i}{\partial (r_i^{mem})^2} > 0$ due to $\alpha > 0$, $\kappa_{i,3} > 0$ and $r_i^{mem} > 0$. From Hessian Matrix, we can derive that $\frac{\partial^2 F_i}{\partial (r_i^{cpu})^2} \frac{\partial^2 F_i}{\partial (r_i^{mem})^2} - \frac{\partial^2 F_i}{\partial r_i^{cpu} \partial r_i^{mem}} \frac{\partial^2 F_i}{\partial r_i^{mem} \partial r_i^{cpu}} > 0$ always hold, which means that F_i is a convex function with respect to r_i^{cpu} and r_i^{mem} . ■

According to Theorem 2, Subproblem **SP1** is strictly convex and thus admits a unique optimum; the optimal (r_i^{cpu}, r_i^{mem}) can be obtained by standard solvers (e.g., Scipy.optimize, fmincon). Moreover, the monotonicity of F_i with respect to r_i^{mem} implies that the optimal memory is $r_i^{mem} = r_i^{max}$ under the sufficient-resource assumption.

As for Subproblem **SP2**, considering the power consumption of container cluster changes with the increase of container number, the objective is to determine the optimal number

of containers for each type of application given the optimal solution of **SP1**. Subproblem **SP2** can be formulated as:

$$\mathbf{SP2:} \min_{N_i} \Phi(N_i) = \alpha W_s(N_i, \lambda_i, \mu_i^*) + \beta \frac{\Delta P(N_i)}{\lambda_i}, \quad (23)$$

$$\text{s.t. } W_s(N_i, \lambda_i, \mu_i^*) = \frac{L_s(N_i, \lambda_i, \mu_i^*)}{\lambda_i}, \quad (24)$$

$$\Delta P(N_i) = (P^{full} - P^{idle}) \frac{N_i r_i^{cpu*}}{R^{cpu}}, \quad (25)$$

where $\Phi(N_i)$ represents the utility of server for application i , μ_i^* denotes the optimal service rate of application container i , which can be derived by Eq.(6) given the optimal solutions of **SP1**. $P(N_i)$ represents the power consumption of deploying N_i containers for application i .

To verify the existence of optimal solution for Subproblem **SP2**, we analyze the convexity of $\Phi(N_i)$ with respect to N_i , which is shown as following:

Theorem 3: $\Phi(N_i)$ is a convex function with respect to N_i .

Proof: It is easy to find that the power consumption function $\Delta P_i(N_i)$ is a linear function with respect to N_i . Thus, the convexity of $\Phi(N_i)$ depends on that of $W_s(N_i, \lambda_i, \mu_i^*)$. Based on [35], it has been proved that $W_s(N_i, \lambda_i, \mu_i^*)$ is a convex function with respect to N_i . Thus, we have that $\Phi(N_i)$ is a convex function with respect N_i . ■

According to Theorem 3, Subproblem **SP2** is a convex one-dimensional optimization and can be solved efficiently via ternary search. For implementation, we define the search interval as

$$N_i \in \left[\left\lceil \frac{\lambda_i}{\mu_i^*} \right\rceil, \min \left\{ \frac{R^{cpu}}{r_i^{cpu*}}, \frac{R^{mem}}{r_i^{mem*}} \right\} \right],$$

where the lower bound enforces queue stability ($\lambda_i \leq N_i \mu_i^*$), and the upper bound is the maximum number of containers the server could host for application i if all CPU and memory resources were devoted to this application. The resulting N_i^* thus captures the *ideal* container count under the sufficient-resource assumption and serves as an upper-bound demand. Based on this per-application analysis, we design an efficient server resource management procedure to solve subproblems **SP1** and **SP2** for M kinds of applications under the sufficient-resource assumption, as shown in Algorithm 1. The constrained intra-node allocation under (9)-(10) is handled by the container-based scheme discussed in the following subsection.

B. Container-based Resource Management Scheme

Algorithm 1 solves the relaxed subproblems **SP1** and **SP2** under sufficient-resource assumptions for each application, yielding an ideal configuration $c_i^* = (r_i^{cpu*}, r_i^{mem*}, N_i^*)$ that represents the upper-bound demand of application i . However, these per-application configurations cannot be directly deployed on a resource-limited edge server because the global CPU and memory constraints (9)-(10) may be violated. To address this limitation, we design a *Container-based Resource Management Scheme* (CRMS) that redistributes resources across heterogeneous applications while maintaining global feasibility. CRMS exploits container elasticity to reallocate CPU and memory resources, reducing them for applications

with low sensitivity to resource changes and assigning more to latency-sensitive ones, thus improving overall utility under constrained conditions.

Algorithm 1 Efficient Server Resource Management in Sufficient Resource Condition

Input: $\overline{R^{cpu}}, \overline{R^{mem}}, \alpha, \beta, \lambda_i, \kappa_{i,1}, \kappa_{i,2}, \kappa_{i,3}, r_i^{min}, r_i^{max}$
Output: $r_i^{cpu*}, r_i^{mem*}, N_i^*$

```

1: for  $i = 1 \rightarrow M$  do
2:   Obtain  $r_i^{cpu*}, r_i^{mem*}$  by Scipy.Optimize;
3:   Derive  $\mu_i^*$  by substituting  $r_i^{cpu*}, r_i^{mem*}$  into Eq.(6);
4:   Let  $l = \left\lceil \frac{\lambda_i}{\mu_i^*} \right\rceil$ ,  $r = \min\{\overline{R^{cpu}}/r_i^{cpu*}, \overline{R^{mem}}/r_i^{mem*}\}$ ;
5:   while  $l < r$  do
6:      $lmid = l + (r - l)/3$ ;
7:      $rmid = r - (r - l)/3$ ;
8:     Calculate  $\Phi(lmid)$  and  $\Phi(rmid)$  by Eq.(23);
9:     if  $\Phi(lmid) \leq \Phi(rmid)$  then
10:       $r = rmid - 1$ ;
11:    else
12:       $l = lmid + 1$ ;
13:    end if
14:   end while
15:    $N_i^* = l$ ;
16: end for

```

To illustrate the motivation behind CRMS, Fig. 5 depicts how container performance varies with allocated resources. When a container is allocated abundant CPU resources (Fig. 5(a)), reducing the CPU quota by u -units leads to only a marginal increase in latency. Conversely, when resources are scarce (Fig. 5(b)), the same u -unit reduction results in a significant latency increase. A similar trend is also observed for memory allocation, though the specific sensitivity pattern differs across applications. This observation underpins the CRMS design: resources are slightly reduced for delay-insensitive applications and reallocated to latency-sensitive ones, thereby improving overall system performance under resource constraints.

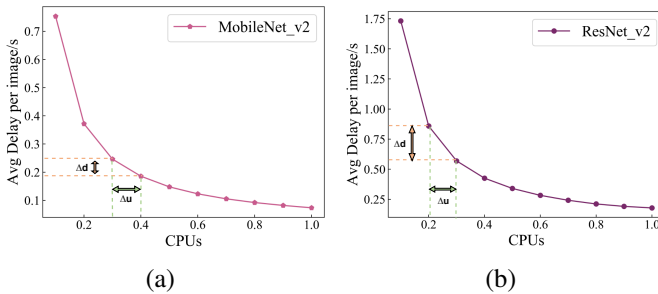


Fig. 5. (a) Container with small delay variation per unit CPU change. (b) Container with large delay variation per unit CPU change.

By effectively balancing per-application resource allocation, the scheme enhances the overall quality of service and ensures that critical applications receive sufficient computational resources. At this point, Problem **P** can be transformed into

Problem **P1**, formulated as

$$\mathbf{P1:} \min_{r_i^{cpu}, r_i^{mem}} \sum_i \left(\alpha W_s(N_i^*, \lambda_i, \mu_i) + \beta \frac{\Delta P(N_i^*)}{\lambda_i} \right), \quad (26)$$

s.t. Constraints.(9) – (11) and (25).

Here N_i^* represents the optimal container number derived by Algorithm 1 under sufficient resources assumption, while r_i^{cpu} and r_i^{mem} are reallocated CPU and memory resources. $\Delta P(N_i^*)$ denotes the incremental power consumption of N_i^* containers for application i . To verify the existence of the optimal resource configuration for Problem **P1**, we analyze the convexity of U_i with respect to r_i^{cpu} and r_i^{mem} as follows.

Theorem 4: U_i is a convex function with respect to the resources r_i^{cpu} and r_i^{mem} when N_i^* is given.

Proof: Based on Constraint (25), $\Delta P_i(N_i^*)$ is linear with respect to resource variables and therefore does not affect convexity. Thus, the convexity of U_i depends on that of $W_s(N_i^*, \lambda_i, \mu_i)$ with respect to the resources r_i^{cpu} and r_i^{mem} . According to [36], in an M/M/N queuing system, it has been proven that $\frac{\partial W_s(N_i^*, \lambda_i, \mu_i)}{\partial \rho_i} > 0$ and $\frac{\partial^2 W_s(N_i^*, \lambda_i, \mu_i)}{\partial (\rho_i)^2} > 0$, where $\rho_i = \frac{\lambda_i}{N_i^* \mu_i}$. Using Eq. (6), ρ_i is further represented as $\frac{\lambda_i \bar{x}_i d_i}{N_i^*}$, with λ_i , \bar{x}_i , and N_i being constants in Problem **P1**. From this expression, we can derive that $\frac{\partial \rho_i}{\partial r_i^{cpu}} < 0$, $\frac{\partial \rho_i}{\partial r_i^{mem}} < 0$ and $\frac{\partial^2 \rho_i}{\partial (r_i^{cpu})^2} > 0$ according to Theorem 3. Applying the chain rule, we can obtain the second derivative of $W_s(N_i^*, \lambda_i, \mu_i)$ with respect to r_i^{cpu} and r_i^{mem} , i.e.,

$$\frac{\partial^2 W_s}{\partial (r_i^{cpu})^2} = \frac{\partial^2 W_s}{\partial (\rho_i)^2} \left(\frac{\partial \rho_i}{\partial r_i^{cpu}} \right)^2 + \frac{\partial^2 \rho_i}{\partial (r_i^{cpu})^2} \frac{\partial W_s}{\partial \rho_i} > 0, \quad (27)$$

$$\frac{\partial^2 W_s}{\partial (r_i^{mem})^2} = \frac{\partial^2 W_s}{\partial (\rho_i)^2} \left(\frac{\partial \rho_i}{\partial r_i^{mem}} \right)^2 + \frac{\partial^2 \rho_i}{\partial (r_i^{mem})^2} \frac{\partial W_s}{\partial \rho_i} > 0 \quad (28)$$

and

$$\frac{\partial^2 W_s}{\partial r_i^{cpu} \partial r_i^{mem}} = \frac{\partial^2 W_s}{\partial (\rho_i)^2} \frac{\partial \rho_i}{\partial r_i^{cpu}} \frac{\partial \rho_i}{\partial r_i^{mem}} + \frac{\partial^2 \rho_i}{\partial r_i^{cpu} \partial r_i^{mem}} \frac{\partial W_s}{\partial \rho_i}. \quad (29)$$

From Hessian Matrix, we can derive that $\frac{\partial^2 W_s}{\partial (r_i^{cpu})^2} \cdot \frac{\partial^2 W_s}{\partial (r_i^{mem})^2} - (\frac{\partial^2 W_s}{\partial r_i^{cpu} \partial r_i^{mem}})^2 > 0$ holds, which means that $W_s(N_i^*, \lambda_i, \mu_i)$ is a convex function with respect to r_i^{cpu} and r_i^{mem} . Therefore, U_i is a convex function with respect to r_i^{cpu} and r_i^{mem} given N_i^* . \blacksquare

According to Theorem 4, when the container count N_i^* is given, Problem **P1** is a convex optimization problem over CPU and memory allocations. This provides the theoretical basis for global resource reallocation in constrained edge servers. The optimal solution to **P1** can be efficiently obtained via convex solvers and, together with Algorithm 1, forms the foundation of the proposed CRMS.

Initially, Algorithm 1 computes per-application configurations $c_i^* = (r_i^{cpu*}, r_i^{mem*}, N_i^*)$ under unconstrained conditions (lines 1–2), serving as upper-bound references for Problem **P**. If these configurations exceed the server's total CPU or memory capacities (9)–(10), we fix N_i^* based on Theorem 4 and solve Problem **P1** to reallocate CPU and memory resources (lines 3–7), obtaining feasible configurations c_i' . Then, the

Algorithm 2 Container-based Resource Management Scheme (CRMS)

Require: $\overline{R_{cpu}}$, $\overline{R_{mem}}$, α , β , $\lambda_i, \kappa_{i,1}, \kappa_{i,2}, \kappa_{i,3}, r_i^{min}, r_i^{max}$
Ensure: C

- 1: Compute $c_i^* = (r_i^{cpu*}, r_i^{mem*}, N_i^*)$ for each application via Algorithm 1;
- 2: $C \leftarrow C \cup \{c_i\}$;
- 3: **if** $\sum_i N_i^* r_i^{cpu*} > \overline{R_{cpu}}$ or $\sum_i N_i^* r_i^{mem*} > \overline{R_{mem}}$ **then**
- 4: Given $N'_i = N_i^*, \forall i$
- 5: Solve Problem **P1** to obtain $r_i^{cpu'}, r_i^{mem'}$;
- 6: Update $C = \{c'_i, \forall i\}$ and Calculate U_p by Eq.(8);
- 7: **end if**
- 8: **while** true **do**
- 9: Set $\mathcal{O} \leftarrow \emptyset$;
- 10: **for** $i = 1 \rightarrow M$ **do**
- 11: Set $\hat{N}_i = N'_i - 1$;
- 12: Solve Problem **P1** for $\hat{C} = \{\hat{c}_i, \forall i\}$;
- 13: Calculate \hat{U}_p by Eq.(8);
- 14: $\mathcal{O} \leftarrow \mathcal{O} \cup \{(\hat{U}_p, \hat{C})\}$;
- 15: **end for**
- 16: $U_p^*, C^* \leftarrow \text{argmin}_{(\hat{U}_p, \hat{C}) \in \mathcal{O}} (\hat{U}_p)$;
- 17: **if** $U_p^* < U_p$ **then**
- 18: Update $C \leftarrow C^*$, $U_p \leftarrow U_p^*$;
- 19: **else**
- 20: Break;
- 21: **end if**
- 22: **end while**

overall utility U_p is computed via Eq.(8). Even if the initial configurations satisfy resource constraints, the upper-bound nature of Algorithm 1 may not guarantee global optimality. Hence, a greedy refinement is applied to iteratively decrease N_i for each application, re-solving **P1** at every step (lines 8–22). If a reduced configuration yields a smaller U_p , the update is accepted; otherwise, the process terminates when no further improvement is possible.

Complexity Analysis: The computational complexity of CRMS arises from solving convex optimization problems using the Sequential Least Squares Programming (SLSQP) method in the Scipy.optimize library [37]. Algorithm 1 iteratively determines optimal CPU and memory configurations and the instance count for M applications by solving a convex problem with two decision variables (CPU and memory). The per-application solve costs $O(k_1 \cdot 2^3)$ (where k_1 is the SLSQP iteration count), giving $O(M \cdot k_1 \cdot 2^3)$ across all applications. In addition, the ternary search used to refine N_i contributes $O(M \cdot \log_3(\Delta) \cdot T_\Phi)$, where $\Delta = \min\left\{\frac{\overline{R_{cpu}}}{r_i^{cpu*}}, \frac{\overline{R_{mem}}}{r_i^{mem*}}\right\} - \left\lceil \frac{\lambda_i}{\mu_i^*} \right\rceil$ denotes the search range induced by queue stability and the server's CPU/memory budgets, and T_Φ is the cost of evaluating $\Phi(\cdot)$ (including computing W_s via Eq. (7)). Hence, Algorithm 1 has complexity $O(M \cdot (k_1 \cdot 2^3 + \log_3(\Delta) \cdot T_\Phi))$. Algorithm 2 then proceeds in two phases: Phase 1 invokes Algorithm 1, and Phase 2 refines allocations by repeatedly solving Problem **P1** with $2M$ decision variables (CPU and memory for all applications), each with a per-solve cost of $O(k_2 \cdot (2M)^3)$, where k_2 is the number of iterations in the SLSQP solver. Over K refine-

ment iterations, solving M instances of **P1** per iteration incurs $O(K \cdot M \cdot k_2 \cdot (2M)^3)$, so the total complexity of Algorithm 2 is $O(M \cdot (k_1 \cdot 2^3 + \log_3(\Delta) \cdot T_\Phi) + K \cdot M \cdot k_2 \cdot (2M)^3)$, dominated by $O(M \cdot k_1 \cdot 2^3)$ and $O(K \cdot M \cdot k_2 \cdot (2M)^3)$.

In practice, CRMS operates in a quasi-dynamic manner: the allocator re-executes Algorithm 2 only when the monitor detects significant changes in the arrival rates $\{\lambda_i\}$ or in the active application mix, while container quotas remain fixed between optimization cycles. Thus, each optimization cycle incurs the polynomial-time complexity derived above. The re-optimization overhead scales with the number of applications and adaptation events, rather than with the per-request workload, making CRMS suitable for practical online use under global constraints (9)–(10).

VI. SIMULATION AND EXPERIMENTS

To evaluate the performance of the proposed scheme, we conduct extensive simulations from two perspectives. One is to evaluate the efficiency of the proposed scheme by comparing it to other existing schemes. The other is to analyze the impact of system parameters on performance in terms of processing delay and power consumption.

The simulation environment is implemented in Python and executed on an Intel(R) Core(TM) i7-9700 processor. Simpy is used to simulate the task request process, while scipy.optimize is employed to solve the optimization problem. The experimental setup is defined as follows. Based on the profiling results in Section III, we consider $M = 4$ applications, comprising three image classification tasks implemented using the ResNet_v2, SE_ResNeXt, and MobileNet_v2 models, and one object detection task implemented using the SSD_MobileNet_v1 model. The minimum and maximum memory allocations for the four applications are set as $r^{min} = \{200, 200, 150, 330\}$ MB, $r^{max} = \{400, 400, 350, 700\}$ MB, respectively. The total available CPUs and memory resources range within $\overline{R_{cpu}} \in [28, 38]$, $\overline{R_{mem}} \in [6.5, 11]$ GB, respectively. For each application $i \in M$, the arrival rate λ_i and the average number of images per request x_i follow $\lambda_i \in [4, 15]$, $x_i \in [4, 8]$. The task arrivals for each application follow a Poisson distribution, and the number of images per request is modeled using an exponential distribution. The weight parameters for processing delay and power consumption are set as $\alpha = 1.4$, $\beta = 0.2$, respectively. To simplify the description, we refer to ResNet_v2, SE_ResNeXt, MobileNet_v2 and SSD_MobileNet_v1 as APP1, APP2, APP3 and APP4, respectively.

A. Performance Compared to Schemes

As analyzed in Section V-B, the amount of available resources on the edge server determines the outcome of the resource management strategy. Based on this observation, we conduct comparative experiments under both sufficient and constrained resource conditions.

Under sufficient resource conditions: to highlight the impact of task heterogeneity on CPU and memory allocation, we compare our approach with a method called **SNFC**, which dynamically scales the number of pods while keeping their resource configurations fixed. Unlike our approach, existing

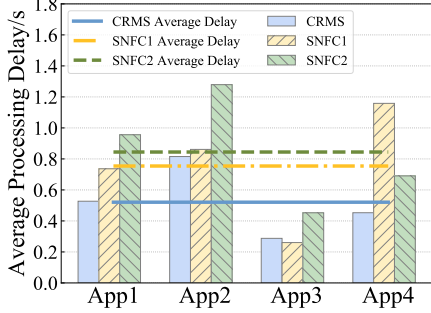


Fig. 6. Comparison of avg processing delay.

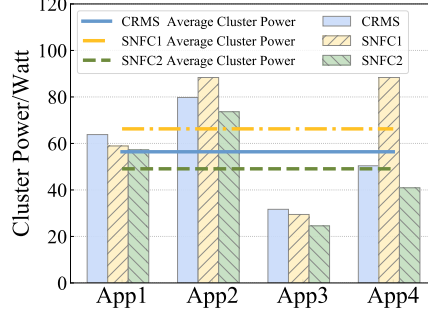


Fig. 7. Comparison of power consumption.

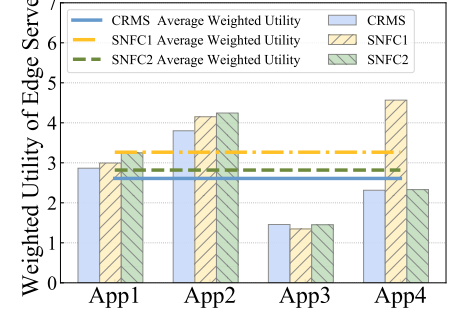


Fig. 8. Comparison of the edge server utility.

methods such as [6] often overlook the varying sensitivities of tasks to CPU and memory resources. This omission makes it difficult to configure resources optimally for diverse applications, resulting in degraded quality of service (QoS). For comparison, we set up two configurations of SNFC: **SNFC1** with $r^{cpu} = 1.8$ and $r^{mem} = 350$, and **SNFC2** with $r^{cpu} = 1$ and $r^{mem} = r^{max}$. With $\lambda_i = 6$ and $x_i = 5, \forall i \in M$, the comparative results are presented below.

In Figs. 6-7, the CRMS algorithm achieves the lowest average processing delay across all four applications, while maintaining the second-lowest power consumption. This is due to its ability to dynamically allocate container and CPU resources according to the specific demands of each application. Although CRMS leads to slightly higher power consumption compared to SNFC2, it achieves a more effective trade-off between resource utilization and performance, particularly in reducing processing delays. According to Theorem 2, the processing delay exhibits a convex relationship with respect to CPU and memory resources. This means that while increasing both CPU and memory resources proportionally can help reduce latency, it does not necessarily result in optimal resource allocation. Therefore, simply increasing the number of containers may not always minimize the processing delay, as demonstrated in Fig. 6. Additionally, Fig. 8 shows the edge utility, defined as the weighted average of processing delay and power consumption. CRMS achieves the lowest edge utility, indicating that it offers the best overall balance between delay reduction and power efficiency, outperforming both SNFC1 and SNFC2 in terms of overall system performance.

Given the container resource bounds defined by r^{min} and r^{max} , SNFC1 exhibits a different behavior. While it satisfies the memory requirements for APP3, it struggles with APP2 and APP4 due to its limited memory allocation. APP2 is highly sensitive to memory availability, and even a slight undersupply of memory leads to significant increases in delay. In such cases, SNFC1 must allocate additional containers to compensate, thereby increasing both memory consumption and processing delay. In contrast, although APP4 is less sensitive to memory fluctuations, it requires a relatively large memory allocation to maintain efficient performance. When memory allocation is insufficient, APP4 experiences elevated delays. To meet performance demands, SNFC1 needs to open a larger number of containers, which results in increased CPU usage and higher power consumption, as shown in Fig. 7. The higher

CPU usage observed in SNFC1, particularly for APP4, reflects inefficient resource utilization, as illustrated in Fig. 9.

SNFC2 adopts a different strategy by allocating sufficient memory to all applications, thereby avoiding the performance degradation observed in memory-sensitive applications such as APP2. This sufficient memory provisioning prevents significant performance degradation. Consequently, SNFC2 exhibits the highest memory usage, as shown in Fig. 10. However, the CPU allocation per container in SNFC2 is slightly insufficient, leading to increased delays across all applications, as depicted in Fig. 6. Due to the linear relationship between CPU usage and power consumption, SNFC2 achieves lower power consumption compared to CRMS, as depicted in Fig. 7. However, the under-provisioned CPU resources compel SNFC2 to deploy a larger number of containers for compensation, thereby reducing overall resource efficiency. Although SNFC2 achieves better power efficiency, its increased number of containers results in excessive memory usage and inefficient CPU utilization, highlighting an imbalance in resource allocation.

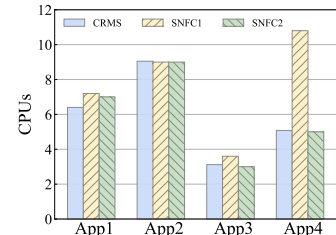


Fig. 9. Comparison of CPU usage.

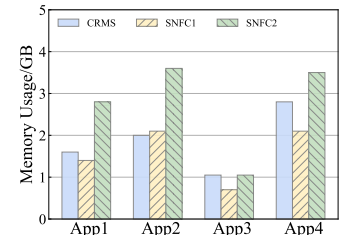


Fig. 10. Comparison of Mem usage.

In contrast, CRMS dynamically adjusts both CPU and memory resources according to the specific needs of each application, ensuring a better trade-off between delay reduction and resource efficiency. Figs. 9 and 10 highlight how CRMS minimizes both CPU and memory overhead compared to the inefficiencies observed in SNFC1 and SNFC2. This dynamic resource allocation mechanism enables CRMS to achieve the lowest edge utility, demonstrating its effectiveness in managing heterogeneous application demands while optimizing both performance and resource utilization.

Under constrained resource conditions: we evaluate the effectiveness of CRMS's elastic scaling mechanism by comparing it with other baseline methods, given fixed total server resources. The comparison includes the following schemes:

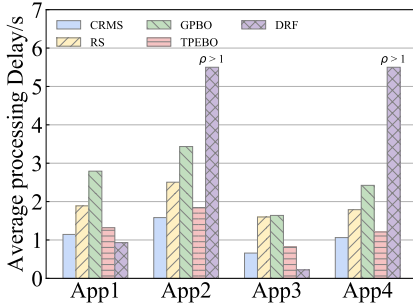


Fig. 11. Comparison of processing delay.

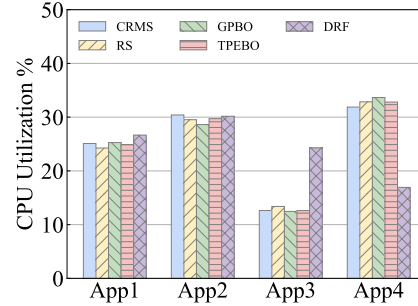


Fig. 12. Comparison of CPU utilization.

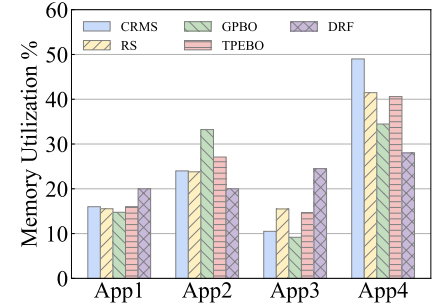


Fig. 13. Comparison of memory utilization.

- Random Search (**RS**) [38]: A baseline hyperparameter optimization method that samples configurations randomly from the parameter space, offering a straightforward benchmark for evaluating advanced algorithms.
- Gaussian Process Bayesian Optimization (**GPBO**) [39]: Builds a probabilistic model using Gaussian processes to identify promising configurations with fewer evaluations, suitable for costly optimization tasks such as container resource allocation.
- Tree-structured Parzen Estimator Bayesian Optimization (**TPEBO**) [40]: Separately models good and bad configuration distributions to guide the search process. It is well-suited for our tree-structured problem involving container count selection and CPU/memory allocation.
- Dominant Resource Fairness (**DRF**) [41]: Ensures fair multi-resource allocation (e.g., CPU and memory) by equalizing dominant resource shares across tasks, promoting balanced resource usage in containerized environments.

The performance of the proposed CRMS scheme is evaluated against these algorithms to demonstrate its effectiveness in jointly optimizing container counts and resource allocations, particularly in heterogeneous and resource-constrained environments. From Eq.(3), the power consumption can be regarded as the constant given the total CPUs. Thus, we mainly compare the delay performance of CRMS, RPA, and DRF. By setting $\lambda_1 = 8, \lambda_2 = 7, \lambda_3 = 10, \lambda_4 = 15, x_i = 5, \forall i \in M, R^{cpu} = 30, R^{mem} = 10GB$, the comparative results are shown as follows.

As shown in Fig. 11, the CRMS, RS, GPBO, and TPEBO algorithms all successfully find feasible resource allocation schemes under constrained resource conditions. Notably, CRMS achieves the lowest average latency, reducing it by 43%, 57%, and 14% compared to the other methods, respectively. Figs. 12-13 further demonstrate that CRMS handles the varying sensitivities of heterogeneous tasks to CPU and memory more effectively. This advantage arises because GPBO and TPEBO, constrained by the limited number of iterations, may not sufficiently explore the large parameter space, thereby making it challenging to converge on the optimal resource allocation. RS, by contrast, performs a random search across the entire parameter space without leveraging prior knowledge, which decreases the likelihood of finding an optimal solution.

The proposed CRMS starts with an initial resource allocation derived under unconstrained conditions and then iteratively

adjusts the CPU and memory allocations for containers using a greedy approach to refine the configuration with fewer iterations. In comparison, the DRF algorithm prioritizes resources for applications with high demands, leading to resource shortages for other applications. This imbalance results in the task queues for APP2 and APP4 exceeding their capacity ($\rho > 1$), indicating that these queues cannot be maintained within stable bounds. This comparison with DRF further underscores the importance of considering task heterogeneity in resource allocation strategies. Neglecting this factor may prevent certain applications from meeting their service requirements, often necessitating task offloading to other edge servers and thereby undermining the effective utilization of local computational resources.

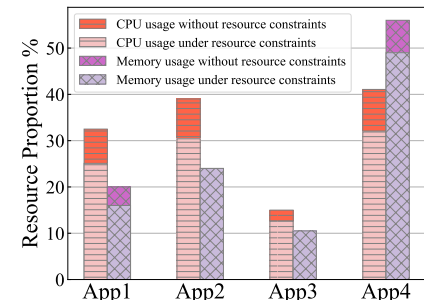


Fig. 14. Results of resource reallocation under resource constraints

To verify the effectiveness of resource reallocation, we illustrate the changes in CPU and memory usage after incorporating resource constraints in Fig. 14. The CRMS algorithm initially solves the resource allocation problem without constraints to obtain a preliminary solution, which is then iteratively refined under resource constraints. As a result, the system adjusts resource allocation based on the heterogeneous resource demands of different applications.

For CPU resources, all four applications undergo varying degrees of adjustment compared to the unconstrained scenario. The extent of CPU reallocation differs across applications, reflecting their sensitivity to computational resource constraints. In contrast, memory adjustments are primarily applied to APP1 and APP4, while APP2 and APP3 retain their original memory configurations. Additionally, the degree of memory reallocation varies between APP1 and APP4, highlighting the system's ability to selectively compress memory resources where necessary while ensuring sufficient allocation for applications with higher memory demands.

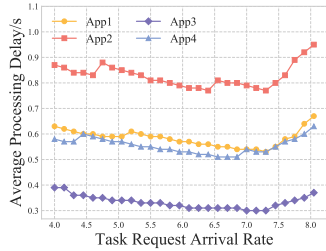


Fig. 15. Processing delay with different task arrival rates.

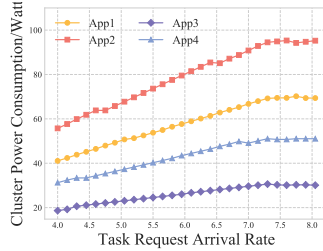


Fig. 16. Power consumption with different task arrival rates.

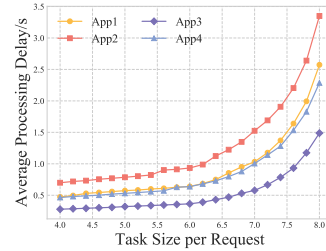


Fig. 17. Processing delay under different request workloads.

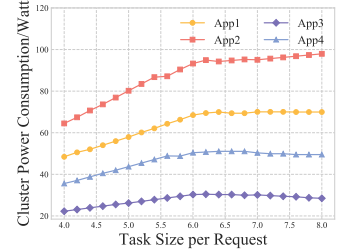


Fig. 18. Power consumption under different request workloads.

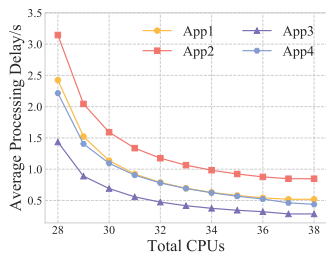


Fig. 19. Processing delay for different CPU resources.

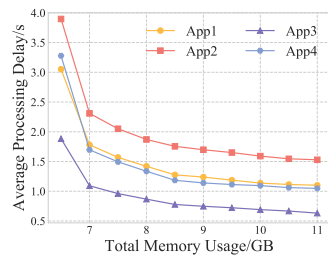


Fig. 20. Processing delay for different memory resources.

B. Analysis of System Parameters

Since the optimal results can be affected by system parameters, we analyze their impact from three aspects: 1) The task arrival rate λ_i , which reflects the performance of CRMS in processing delay and power consumption under varying workloads, as shown in Figs.15-16; 2) The average number of images per request x_i , which characterizes the computational workload per request and influences the system's service capacity and delay performance, as shown in Figs.17-18; 3) The upper bounds of CPU and memory resources (\bar{R}^{cpu} , \bar{R}^{mem}), which help assess the delay performance of CRMS under resource-constrained conditions through resource reallocation, as shown in Figs.19-20.

The impact of λ_i : As shown in Fig. 15, the processing delay decreases as the task arrival rate (λ_i) increases, under the conditions of $\bar{R}^{cpu} = 30$, $\bar{R}^{mem} = 10GB$, and $x_i = 5$. This trend occurs because the optimization objective defined in Equation (8) incorporates the time-averaged power consumption per request. As λ_i increases, the relative weight of power consumption in the optimization objective diminishes, allowing the system to prioritize delay reduction. During this phase, CRMS dynamically adjusts resource allocation to optimize delay, resulting in an overall reduction in processing time.

Additionally, periodic fluctuations in the delay curve are observed in Fig.15, caused by CRMS activating additional containers to enhance parallelism when the CPU and memory resources of existing containers become insufficient. This reconfiguration temporarily reduces the resources allocated to each container, causing a slight increase in delay before the system stabilizes. As λ_i approaches 7, server resources become constrained, intensifying competition among applications. At this stage, CRMS reallocates resources based on application sensitivity. Resource-intensive applications, such as APP2,

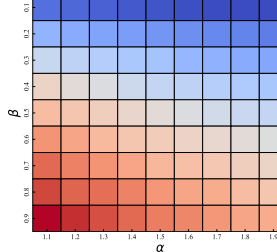


Fig. 21. The impact of α , β on processing delay.

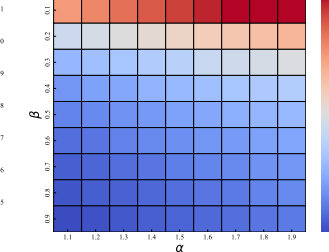


Fig. 22. The impact of α , β on power consumption.

experience increased delay due to higher contention, while lightweight applications like APP3 maintain relatively stable performance under constrained conditions. This mechanism allows CRMS to mitigate the impact of resource contention, delaying overall performance degradation. Fig.16 shows that during the resource-sufficient phase, cluster power consumption increases steadily as more containers are activated. Beyond $\lambda_i = 7$, the power consumption plateaus, indicating full utilization of server resources. At this point, CRMS redistributes resources among existing containers based on application sensitivity, ensuring efficient resource use while minimizing delay increases.

The impact of x_i : as shown in Fig.17, under the condition of $\bar{R}^{cpu} = 30$, $\bar{R}^{mem} = 10GB$, and $\lambda_i = 6$, the processing delay of the four applications remains relatively stable as the request workload (x_i) increases, until x_i exceeds approximately 6. During this phase, CRMS dynamically adjusts CPU and memory allocations for containers to handle the growing task size efficiently. However, when x_i surpasses 6, the delay for all applications begins to rise significantly, indicating that server resources have reached their limit and resource contention intensifies. The trends in delay reveal the influence of resource sensitivity. For higher resource-demanding applications, such as APP2, the delay increases more steeply after saturation, whereas applications like APP3, with lower resource demands, experience a slower increase in delay. This disparity occurs because CRMS reallocates resources dynamically by compressing allocations for less resource-sensitive applications (e.g., App1, App3, and App4) to support applications like App2, which require more resources to maintain performance. Fig.18 shows a corresponding trend in power consumption. Initially, power consumption increases steadily with x_i as additional containers are activated and resources are allocated to meet task demands. After x_i reaches 6, power consumption

reaches a plateau for most applications, reflecting the server's full utilization. Notably, App2's power consumption continues to rise, demonstrating that CRMS prioritizes its resource adjustments to accommodate higher task sizes for resource-intensive applications, even under constrained conditions.

The impact of $\overline{R^{cpu}}$ and $\overline{R^{mem}}$: as shown in Fig. 19, under the experimental conditions where the task arrival rates (λ_i) for the four applications are 8, 7, 10, and 15, and the task size per request (x_i) is fixed at 5, the processing delay decreases non-linearly as $\overline{R^{cpu}}$ increases, with $\overline{R^{mem}}$ fixed at 10GB. For resource-intensive applications such as App2, the reduction in processing delay is more pronounced due to their higher demand for computational resources. Increasing $\overline{R^{cpu}}$ allows the system to allocate more CPU resources to unit containers or activate additional containers, effectively reducing resource contention. In contrast, lighter applications like App3 exhibit a gentler delay reduction curve, reflecting their lower sensitivity to increases in CPU resources. Fig. 20 shows the variation in processing delay with $\overline{R^{mem}}$, while fixing $\overline{R^{cpu}}$ at 30. The processing delay also decreases non-linearly as memory resources increase. Applications with higher memory requirements, such as APP2 and APP4, show significant improvements in delay reduction as $\overline{R^{mem}}$ grows, due to the enhanced ability to buffer and process tasks in parallel. Conversely, App3 shows minimal delay reduction, as its lower memory demands make it less affected by increases in memory capacity.

The impact of α and β : The heatmaps in Fig. 21 and Fig. 22 demonstrate the combined effects of α and β on average processing delay (in seconds) and average power consumption (in watts), highlighting their overall trends. From the first heatmap, the average processing delay increases with β for all values of α , while α itself plays a subtle role, with higher α values generally resulting in slightly reduced delays at the same β . This indicates that β primarily governs the delay, with α introducing secondary adjustments. Conversely, the second heatmap shows that average power consumption decreases as β increases, with higher α values further reducing power consumption, especially when β is large. The trend suggests that higher α and β values improve energy efficiency at the expense of increased processing delay, while lower values of α and β result in reduced delay but higher power consumption. The balance between α and β highlights their complementary roles, where β predominantly dictates the trade-off between delay and energy consumption, and α modulates this effect. These trends emphasize the necessity of jointly tuning α and β to meet application-specific requirements, offering a pathway to balance computational efficiency and energy savings.

VII. CONCLUSION

This study addressed intra-node resource orchestration for heterogeneous edge workloads by integrating empirical latency profiling with a container-level performance model and a queueing-based delay formulation. The resulting joint latency-energy optimization was formulated as a mixed-integer nonlinear program and shown to be computationally intractable. To make the problem solvable in practice,

we decomposed it into tractable convex subproblems and designed a two-stage container-based resource management scheme (CRMS) that jointly configures container counts and CPU/memory quotas under global resource constraints. The scheme exhibits polynomial-time complexity per optimization cycle and supports quasi-dynamic reallocation triggered by workload changes, thereby reconciling theoretical tractability with practical applicability on a single edge server.

Extensive simulations confirmed tangible improvements in both latency and energy efficiency over heuristic and search-based baselines across diverse heterogeneous workloads, validating the proposed model-algorithm co-design. While this work focused on intra-node optimization, the modeling and optimization framework is readily extensible to multi-node edge-cloud settings by incorporating inter-server bandwidth limits, routing decisions, and end-to-end service requirements, as well as temporal adaptation for time-varying demand.

REFERENCES

- [1] Q. Xia, W. Ren, Z. Xu, X. Wang, and W. Liang, "When edge caching meets a budget: Near optimal service delivery in multi-tiered edge clouds," *IEEE Transactions on Services Computing*, vol. 15, no. 6, pp. 3634–3648, 2022.
- [2] Y. Liang, J. Ge, S. Zhang, J. Wu, L. Pan, T. Zhang, and B. Luo, "Interaction-oriented service entity placement in edge computing," *IEEE Transactions on Mobile Computing*, vol. 20, no. 3, pp. 1064–1075, 2021.
- [3] S. Long, C. Wang, W. Long, H. Liu, Q. Deng, and Z. Li, "An efficient task scheduling algorithm in the cloud and edge collaborative environment," *Chinese Journal of Electronics*, vol. 33, no. 5, pp. 1296–1307, 2024.
- [4] F. Rossi, V. Cardellini, F. L. Presti, and M. Nardelli, "Dynamic multi-metric thresholds for scaling applications using reinforcement learning," *IEEE Transactions on Cloud Computing*, vol. 11, no. 2, pp. 1807–1821, 2022.
- [5] N. Mahmoudi and H. Khazaei, "Performance modeling of metric-based serverless computing platforms," *IEEE Transactions on Cloud Computing*, vol. 11, no. 2, pp. 1899–1910, 2023.
- [6] Z. Cai and R. Buyya, "Inverse queuing model-based feedback control for elastic container provisioning of web systems in kubernetes," *IEEE Transactions on Computers*, vol. 71, no. 2, pp. 337–348, 2022.
- [7] J. Cai, B. Chen, J. Wen, Z. Cui, J. Chen, and W. Zhang, "A joint vehicular device scheduling and uncertain resource management scheme for federated learning in internet of vehicles," *Information Sciences*, vol. 690, p. 121552, 2025.
- [8] H. Li, C. Xu, Z. Zhao, and M. Liu, "A multi-granularity task scheduling method for heterogeneous computing resources," *Chinese Journal of Electronics*, 2024.
- [9] J. Wang, C. Cao, J. Wang, K. Lu, A. Jukan, and W. Zhao, "Optimal task allocation and coding design for secure edge computing with heterogeneous edge devices," *IEEE Transactions on Cloud Computing*, vol. 10, no. 4, pp. 2817–2833, 2022.
- [10] W. Shen, W. Lin, W. Wu, H. Wu, and K. Li, "Reinforcement learning-based task scheduling for heterogeneous computing in end-edge-cloud environment," *Cluster Computing*, vol. 28, no. 3, p. 179, 2025.
- [11] J. Feng, W. Zhang, Q. Pei, J. Wu, and X. Lin, "Heterogeneous computation and resource allocation for wireless powered federated edge learning systems," *IEEE Transactions on Communications*, vol. 70, no. 5, pp. 3220–3233, 2022.
- [12] H. Li, J. Xia, W. Luo, and H. Fang, "Cost-efficient scheduling of streaming applications in apache flink on cloud," *IEEE Transactions on Big Data*, vol. 9, no. 4, pp. 1086–1101, 2022.
- [13] Y. Lei, Z. Cai, X. Li, and R. Buyya, "State space model and queueing network based cloud resource provisioning for meshed web systems," *IEEE Transactions on Parallel and Distributed Systems*, vol. 33, no. 12, pp. 3787–3799, 2022.
- [14] Y. Xie, M. Jin, Z. Zou, G. Xu, D. Feng, W. Liu, and D. Long, "Real-time prediction of docker container resource load based on a hybrid model of arima and triple exponential smoothing," *IEEE Transactions on Cloud Computing*, vol. 10, no. 2, pp. 1386–1401, 2022.

[15] L. Toka, G. Dobreff, B. Fodor, and B. Sonkoly, "Machine learning-based scaling management for kubernetes edge clusters," *IEEE Transactions on Network and Service Management*, vol. 18, no. 1, pp. 958–972, 2021.

[16] S. Wang, Z. Ding, and C. Jiang, "Elastic scheduling for microservice applications in clouds," *IEEE Transactions on Parallel and Distributed Systems*, vol. 32, no. 1, pp. 98–115, 2021.

[17] T. Sharif, L. T. Jung, I. Razzak, and M. Alazab, "Adaptive and priority-based resource allocation for efficient resources utilization in mobile-edge computing," *IEEE Internet of Things Journal*, vol. 10, no. 4, pp. 3079–3093, 2023.

[18] Z. He, Y. Sun, B. Wang, S. Li, and B. Zhang, "Cpu–gpu heterogeneous computation offloading and resource allocation scheme for industrial internet of things," *IEEE Internet of Things Journal*, vol. 11, no. 6, pp. 11152–11164, 2024.

[19] X. Zhong, J. Zhang, Y. Zhang, Z. Guan, and Z. Wan, "Pacc: Proactive and accurate congestion feedback for rdma congestion control," in *IEEE INFOCOM 2022-IEEE Conference on Computer Communications*, pp. 2228–2237, IEEE, 2022.

[20] P. Chanfreut, J. M. Maestre, F. J. Muros, and E. F. Camacho, "Clustering switching regions for feedback controllers: A convex approach," *IEEE Transactions on Control of Network Systems*, vol. 8, no. 4, pp. 1730–1742, 2021.

[21] I. Lujic, V. De Maio, S. Venugopal, and I. Brandic, "Sea-leap: Self-adaptive and locality-aware edge analytics placement," *IEEE Transactions on Services Computing*, vol. 15, no. 2, pp. 602–613, 2022.

[22] X. Pang, Z. Wang, J. Li, R. Zhou, J. Ren, and Z. Li, "Towards online privacy-preserving computation offloading in mobile edge computing," in *IEEE INFOCOM 2022-IEEE Conference on Computer Communications*, pp. 1179–1188, IEEE, 2022.

[23] S. Kardani-Moghadam, R. Buyya, and K. Ramamohanarao, "Adrl: A hybrid anomaly-aware deep reinforcement learning-based resource scaling in clouds," *IEEE Transactions on Parallel and Distributed Systems*, vol. 32, no. 3, pp. 514–526, 2020.

[24] L. Han, Z. Yu, Z. Yu, L. Wang, H. Yin, and B. Guo, "Online organizing large-scale heterogeneous tasks and multi-skilled participants in mobile crowdsensing," *IEEE Transactions on Mobile Computing*, vol. 22, no. 5, pp. 2892–2909, 2023.

[25] O. Ascigil, A. G. Tasiopoulos, T. K. Phan, V. Sourlas, I. Psaras, and G. Pavlou, "Resource provisioning and allocation in function-as-a-service edge-clouds," *IEEE Transactions on Services Computing*, vol. 15, no. 4, pp. 2410–2424, 2022.

[26] A. Raza, N. Akhtar, V. Isahagian, I. Matta, and L. Huang, "Configuration and placement of serverless applications using statistical learning," *IEEE Transactions on Network and Service Management*, vol. 20, no. 2, pp. 1065–1077, 2023.

[27] G. Safaryan, A. Jindal, M. Chadha, and M. Gerndt, "Slam: Slo-aware memory optimization for serverless applications," in *2022 IEEE 15th International Conference on Cloud Computing (CLOUD)*, pp. 30–39, IEEE, 2022.

[28] J. Dogani and F. Khunjush, "Proactive auto-scaling technique for web applications in container-based edge computing using federated learning model," *Journal of Parallel and Distributed Computing*, vol. 187, p. 104837, 2024.

[29] T. Shi, H. Ma, G. Chen, and S. Hartmann, "Auto-scaling containerized applications in geo-distributed clouds," *IEEE Transactions on Services Computing*, 2023.

[30] J. Zhang, X. Zhou, T. Ge, X. Wang, and T. Hwang, "Joint task scheduling and containerizing for efficient edge computing," *IEEE Transactions on Parallel and Distributed Systems*, vol. 32, no. 8, pp. 2086–2100, 2021.

[31] S. Tuli, S. R. Poojara, S. N. Srivama, G. Casale, and N. R. Jennings, "Cosco: Container orchestration using co-simulation and gradient based optimization for fog computing environments," *IEEE Transactions on Parallel and Distributed Systems*, vol. 33, no. 1, pp. 101–116, 2022.

[32] P. Pawar and A. Trivedi, "Joint uplink-downlink resource allocation for d2d underlying cellular network," *IEEE Transactions on Communications*, vol. 69, no. 12, pp. 8352–8362, 2021.

[33] H. Kellerer, U. Pferschy, D. Pisinger, H. Kellerer, U. Pferschy, and D. Pisinger, *Multidimensional knapsack problems*. Springer, 2004.

[34] C. A. Floudas, *Deterministic global optimization: theory, methods and applications*, vol. 37. Springer Science & Business Media, 2013.

[35] M. E. Dyer and L. G. Proll, "On the validity of marginal analysis for allocating servers in m/m/c queues," *Management Science*, vol. 23, no. 9, pp. 1019–1022, 1977.

[36] Y. Zhang, X. Lan, J. Ren, and L. Cai, "Efficient computing resource sharing for mobile edge-cloud computing networks," *IEEE/ACM Transactions on Networking*, vol. 28, no. 3, pp. 1227–1240, 2020.

[37] Y. Song, Y. Liu, Y. Zhang, Z. Li, and G. Shou, "Latency minimization for mobile edge computing enhanced proximity detection in road networks," *IEEE Transactions on Network Science and Engineering*, vol. 10, no. 2, pp. 966–979, 2022.

[38] J. Bergstra and Y. Bengio, "Random search for hyper-parameter optimization," *Journal of machine learning research*, vol. 13, no. 2, 2012.

[39] N. Akhtar, A. Raza, V. Ishakian, and I. Matta, "Cose: Configuring serverless functions using statistical learning," in *IEEE INFOCOM 2020-IEEE Conference on Computer Communications*, pp. 129–138, IEEE, 2020.

[40] G. Yu, P. Chen, Z. Zheng, J. Zhang, X. Li, and Z. He, "Faasdeliver: Cost-efficient and qos-aware function delivery in computing continuum," *IEEE Transactions on Services Computing*, vol. 16, no. 5, pp. 3332–3347, 2023.

[41] E. Meskar and B. Liang, "Fair multi-resource allocation in heterogeneous servers with an external resource type," *IEEE/ACM Transactions on Networking*, vol. 31, no. 3, pp. 1244–1262, 2022.